

International Conference on Space Optics—ICSO 2018

Chania, Greece

9–12 October 2018

Edited by Zoran Sodnik, Nikos Karafolas, and Bruno Cugny



Stray-light measurements on gratings: challenges and limitations

D. Tomuta

V. Kirschner

M. Taccola

M. Miranda

et al.



Straylight measurements on gratings: challenges and limitations

Dana Tomuta*, Volker Kirschner, Matteo Taccola, Micael Miranda, Mathijs Arts
European Space Research and Technology Centre (ESTEC), Keplerlaan 1, PO Box 299, 2200 AG
Noordwijk, NL

ABSTRACT

The measurement of the bi-directional scatter distribution function (BSDF) is a well established process on reflective surfaces and largely also on transmissive optical elements. Such measurements are crucial and frequently used as input to assess the straylight performance of optical space instruments. The straylight performance of grating based spectrometers, such as used in Sentinel-5 or FLEX, is to a large extent driven by the grating itself. Thus, a BSDF characterization of gratings for such spectrometers is necessary early in the spectrometer development. However, performing such measurements on gratings turn out to be challenging for a number of reasons that will be presented and addressed in this paper.

In this paper we address some of the challenges experienced when measuring BSDF at different wavelengths from UV up to SWIR for several type of gratings. Scatterometers are usually designed to measure the BSDF of a single flat optical surface. The particular form or construction of such gratings, for example transmissive gratings with at least two optical interfaces or gratings with optical power, requires a reconfiguration of the classical measurement set-up to minimise the errors in the BSDF characterization. Additionally, there is a difficulty of measuring the near-specular scatter of those components due to the inherent optical aberrations and potentially their curvature. The dispersive property of gratings imposes the use of a very stable and spectrally pure light source for the measurement. We suggest some strategies and configurations to mitigate the above-mentioned difficulties.

Some BSDF measurements on curved and immersed gratings are presented in this paper for illustration.

Keywords: BSDF, scatter, curved and immersed gratings, UV, IR

1. INTRODUCTION

1.1 BSDF

The Bidirectional Scattering Distribution Function (BSDF) describes the directional dependence of the reflected or transmitted optical energy. The BSDF is a fundamental optical property and describes the energy scattered into the reflective (BRDF) and transmissive (BTDF) hemisphere of a scattering surface as a function of the angle of the incident radiation (θ_i) and the scatter angle¹. BSDF has been strictly defined as the ratio of the sample differential radiance to the differential irradiance under the assumption of a collimated beam. Power P in W is used instead of intensity I in watts/m², the value θ_s is the polar angle in the scatter direction measured from reflector normal and Ω is the differential solid angle (measured in steradians) through which dP_s (W) scatters when P_i (W) is incident on the reflector (see Figure 1). The cosine comes from the definition of radiance and may be viewed as a correction from the actual size of the scatter source to the apparent size (projected area) as the viewer rotates away from surface normal. A definition of the BSDF is given in by the following formula and represented in Figure 1.

$$BSDF = \frac{\text{differential_radiance}}{\text{differential_irradiance}} = \frac{dP_s / d\Omega_s}{P_i \cos\theta_i}$$

* dana.tomuta@esa.int; phone +31 715656619; esa.int

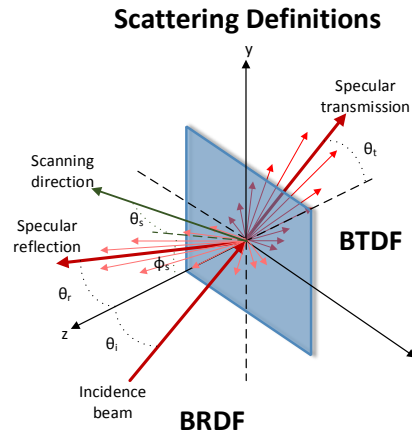


Figure 1. Scattering definitions.

1.2 Scatterometer

The scatterometer used for all BSDF measurements presented in this paper is a commercial scatterometer, Complete Angle Scatter Instrument (CASI). The CASI is a classical scatterometer imaging a point source to a detector at a high F# via the sample under test. The detector aperture and the distance to the sample determine the solid angle for the determination of the BSDF. The optical schematics are presented in Figure 2. Its optical design allows easy accommodation of different light sources, see also Table 1.

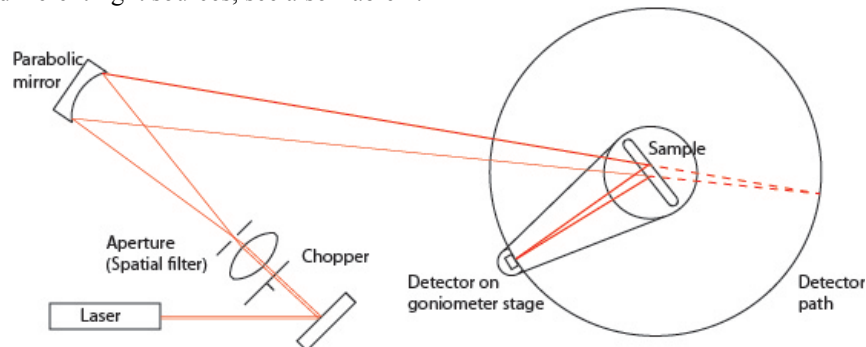


Figure 2. Optical schematics of CASI.

Table 1. CASI scatterometer technical specifications (from manufacturer).

Wavelength:	325 nm, 532 nm, 633 nm, 780nm, 1064 nm, 1.6 μm , 2.3 μm
Noise Equivalent BRDF:	Typical $\sim 10^{-7}$ (wavelength dependent)
Automated Axes:	Resolution 0.001°
	0.01 mm linear
Accuracy:	0.05° angular
	0.01 mm linear
Incident Angle Range:	0 - 85°
Receiver Angle Range:	360°
Sample X/Y motion range:	$\pm 80\text{mm}$
Source/Detector Occulted Area:	$\pm 4^\circ$ around direction of incidence

2. GENERAL ALIGNMENT METHODOLOGY

Before mounting and aligning any type of optical sample into the CASI scatterometer and for each characteristic wavelength, a signature of the instrument is recorded. The signature of the instrument is the intrinsic scatter background without any sample in place and should ideally be as low as possible in order not to introduce errors when measuring an actual sample. The instrument signature at the requested wavelength provides information about the angle-dependent sensitivity of the instrument (noise-floor). For reliable near-specular measurements it is important that the signature drops to levels below the BSDF of the sample under test for small angles from the specular direction, see Figure 3. The central part of the signature is determined by the quasi diffraction-limited imaging performance of the set-up. Aberrations introduced by the off-axis imaging mirror are limited at the operating f-number (~ 100) and have a negligible impact. It should be noted that the instrument signature is wavelength dependent.

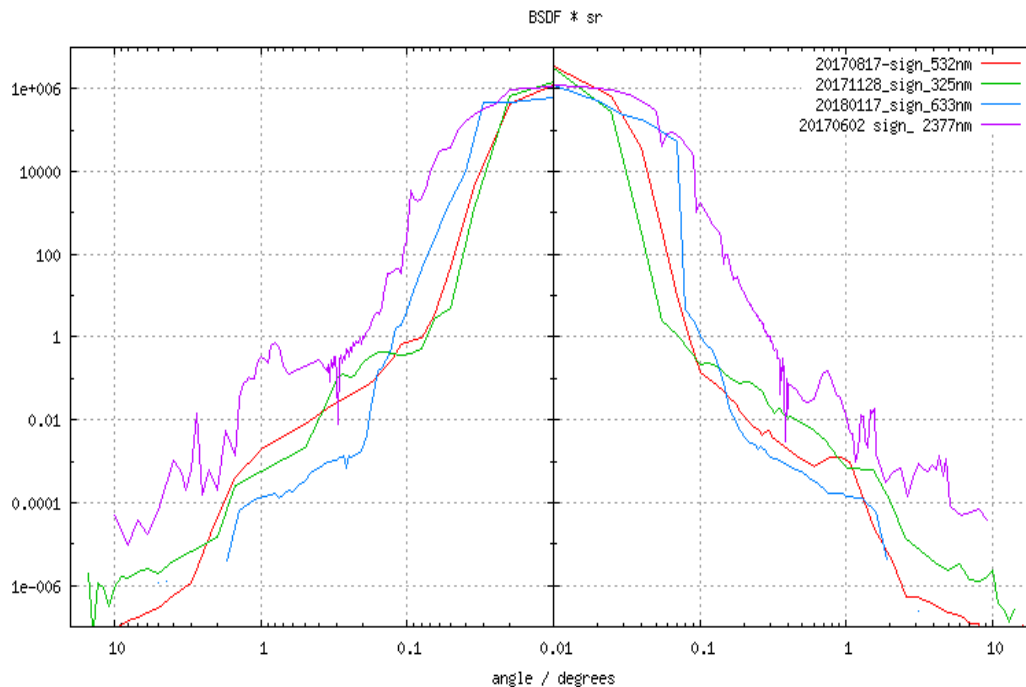


Figure 3. Various signatures of CASI instrument for different wavelengths.

3. MEASUREMENTS: CHALLENGES AND LIMITATIONS

3.1 Near-specular BSDF measurements

Classical BSDF of a flat mirror can be measured down to about 0.1° from specular, according to the above signatures, whereas the situation is different for gratings.

A grating used in the converging beam of the scatterometer in a non-zero diffraction order introduces optical aberrations. A focus contribution can be corrected by adjusting the source position in the set-up, however, higher-order terms unavoidably lead to a larger, aberrated spot on the detector that worsens the near-specular scatter measurement capability. A correction of these aberrations is not possible in the current set-up.

Any change in the set-up, e.g. adjusting the source position, with the purpose of reducing the diffracted aberrated spot, has also disadvantages. When a sample having an optical power is placed at sample stage for BSDF measurement and the source position is changed to reduce the grating aberrations, the signature is no longer valid. The signature of the set-up as presented in Figure 3 loses its validity since it is recorded without any sample in place and at the best focus at the detector position. A second equivalent ‘signature’ within the measurement configuration cannot be recorded and makes

an assessment of the validity of the measurement data close to specular impossible. An optical analysis of the set-up including the test specimen can help to predict the expected impact on the near-specular limit. Alternatively, a simplistic estimation based on the measurement data is possible. Another option is the increase of the f-number for the measurement to even higher values reducing aberrations. The optical chain would eventually be diffraction-limited and the signature measured in the 'empty' set-up remains applicable. However, the measurement spot on the sample becomes very small and the measurement will be sensitive to potential local defects or particles on the sample.

There is an increasing demand to map the straylight as close as possible to the diffraction order of interest, e.g. FLEX gratings². The grating used for FLEX mission³ is a convex grating ($R \approx 200\text{mm}$) and requires an accurate near specular straylight characterization. Figure 4 shows the pattern of the diffracted order of interest having the convex grating mounted on sample stage when using 632.8nm as wavelength. It is not the objective of the present paper to disclose all detailed specifications neither of the grating³ nor of the measurement configuration but rather to underline the challenges of BSDF measurement for such complex optical elements.

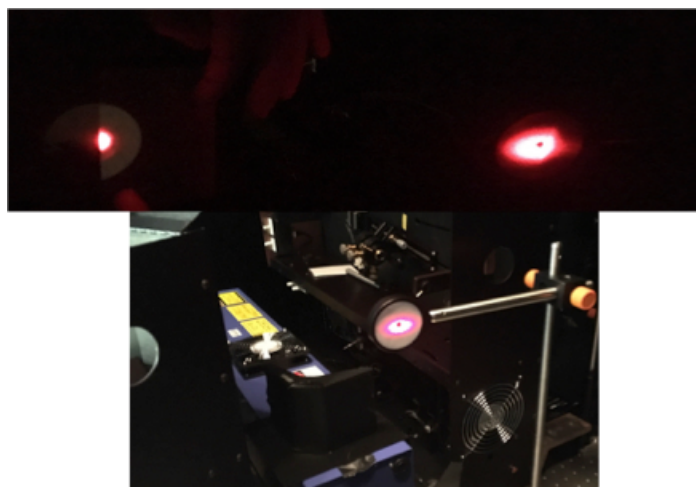


Figure 4. Diffracted beam profile of order of interest for a convex grating when mounted in CASI set-up and before any adjustments.

Depending on the scatterometer limitations, a good compromise between varying several set-up parameters can be found to reduce or compensate such limitations. For the convex grating which diffraction beam profile is shown in Figure 4, two sets of measurements were performed by choosing different angles of incidence in combination with position source adjustment of the set-up. The two different measurement configurations presented in Figure 5 shows the results of such optimizations. All the variables used for the grating's BSDF measurements were a result of Zemax simulation in combination with experience and good knowledge of the set-up capabilities. Note that the near specular region is closer mapped when a smaller goniometer radius and smaller angle of incidence are used in the set-up. BSDF measurements were performed only in the spectral direction.

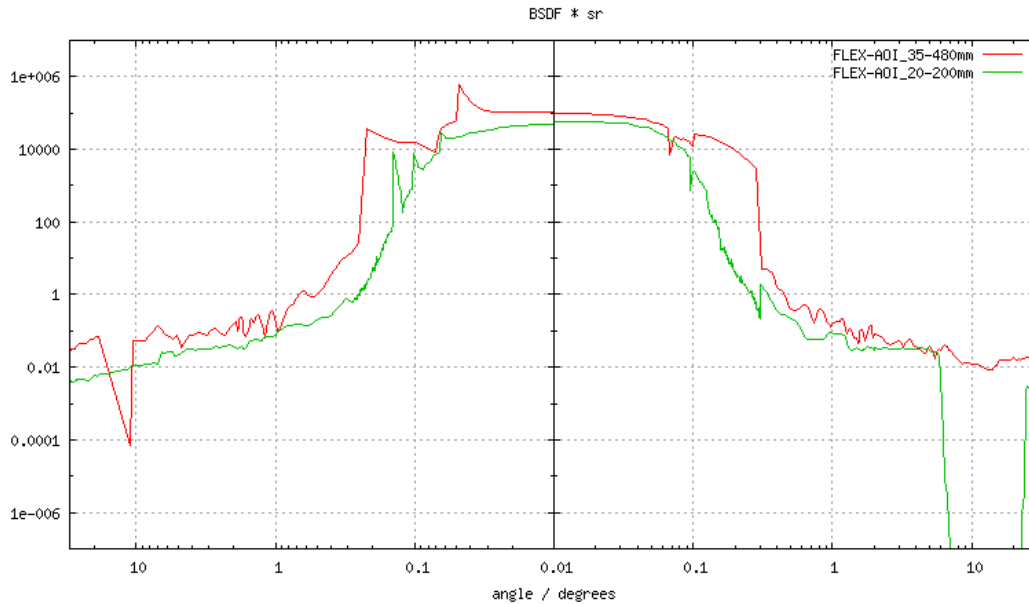


Figure 5. BDF of FLEX convex grating measured in two different configurations. The red line represent the BDF measurement having a larger angle of incidence (AOI=35°) and larger goniometer radius (400mm), whereas the green line represents the BDF measurement having a smaller angle of incidence (AOI=20°) and shorter goniometer radius (200mm). Spurious narrow features seen for the green line are S/W glitches and should be discarded.

Another example of optical complex geometry shape is an immersed grating. The Si-based immersed grating⁴ straylight characterization shows similar challenges as the convex grating presented above, due to the astigmatism induced by the convergent laser beam within the CASI set-up. A solution to overcome such limitation would be to measure with a collimated laser beam. In addition, the immersed grating BDF characterization is requested in IR, at 2377nm. Figure 6 shows the beam profile of the diffracted order of interest for the immersed grating before and after adjusting the CASI set-up. Note that initially, the astigmatic diffracted beam “spot” size was in the range of 14mm whereas after refocusing by adjusting the source position in the set-up, the “spot” size was reduced to less than half.

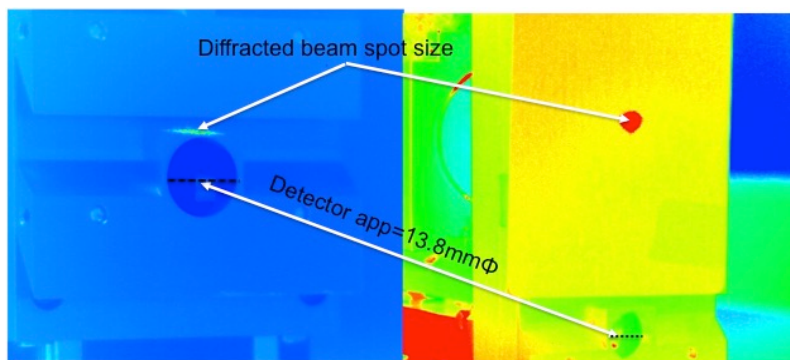


Figure 6. Diffracted beam spot of a Si-based immersed grating using a 2377nm as measurement wavelength.

3.2 Samples anisotropic scattering

The CASI scatterometer can map straylight only in one single scatter plane normal to the goniometer axis. While the BDF is generally a function of θ_i , ϕ_i , θ_s and ϕ_s for most standard and isotropically scattering optical components, a scan

of the BSDF in a single plane is sufficient (usually the plane given by the direction of incidence and the surface normal). Gratings are inherently non-isotropic, which is also reflected in their scatter pattern.

Most of the gratings BSDF are measured for two configurations, in its spectral and spatial direction. This is feasible by measuring the sample in one defined configuration, spectral direction, and then turning the sample by 90° degree and re-measure. More complex geometric gratings, e.g. immersed gratings⁴, need extra theoretical assessment for the exact measurement configuration to map correctly the BSDF in spectral as well as spatial direction. Last but not the least, even if one will measure a grating BSDF in its spectral and across spectral direction, information provided by two direction measurements only, might be insufficient to fully characterize the total straylight of the grating.

The first example chosen in this paper is a GRISM, a prism and a grating ideal combination, measured in transmission at 532nm. Figure 7 shows BSDF measurements of a GRISM around the diffraction order of interest in the spectral direction. As can be noticed, the BSDF spectrum contains multiple extra-features that could be generated by the internal grating reflections. On top of Figure 7 one can visually notice the clear contribution of the multiple extra-features/satellites around the diffraction order of interest, some rings of light beside the presence of localized satellites along the spectral direction. One BSDF measurement only in the spectral plane will contain the overall straylight contributions of all extra-features but not characterizing it correctly. A second measurement is proposed when having the grating slightly clocked/tilted about 5° off from the spectral direction. The second BSDF measurement will map the GRISM straylight not exactly following the spectral direction but slightly off it, by 5°. As some of the extra-features are generated by GRISM internal reflections and contributing only into the spectral direction, it is expected that their amplitude is much reduced or even suppressed when measuring slightly off the spectral direction- see Figure 7. Using the comparison of both BSDF measurements, one can clearly untangle the GRISM straylight from the anisotropic extra-features contribution.

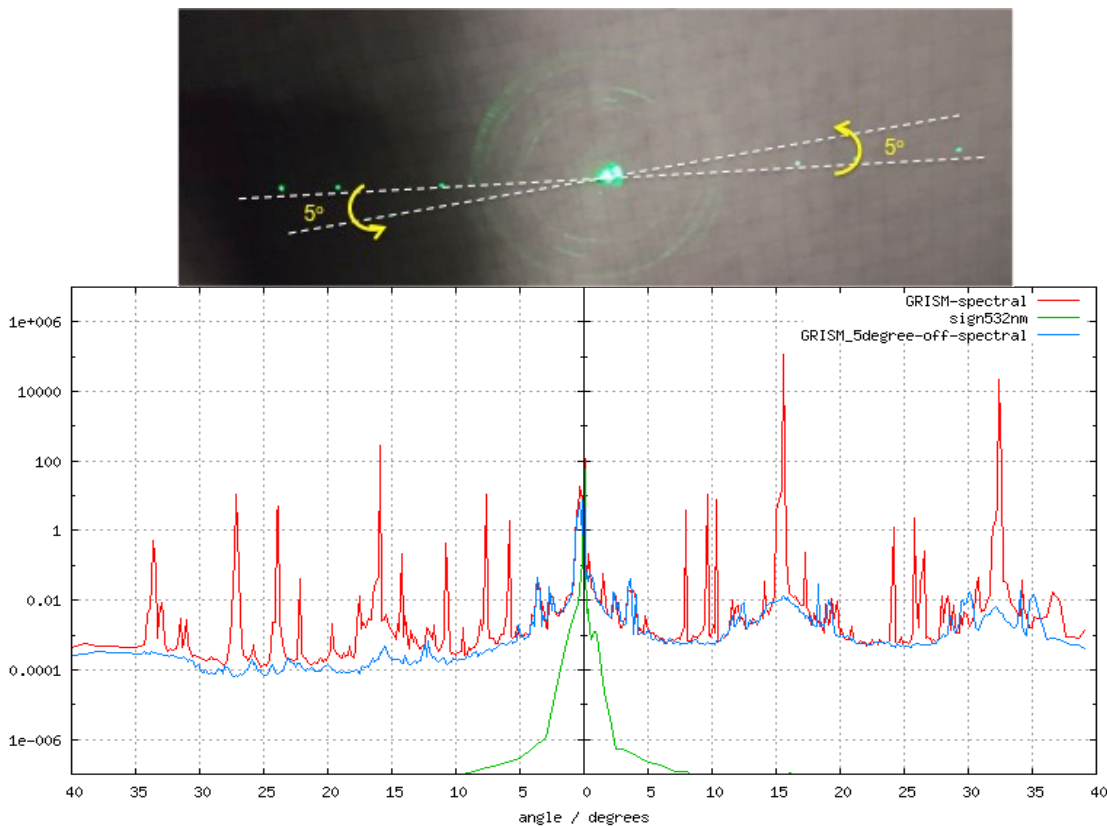


Figure 7. BSDF measurements comparison of GRISM grating at 532nm. Blue BSDF spectra is taken when the grating is clocked 5° off the spectral direction – see top figure.

Second example shown in this section is the same immersed grating presented above, measured at 2377nm (using a band-pass filter). As mentioned earlier, when an IR measurement wavelength is needed, it is no longer easy to visualize

any extra features, even using a high performance IR camera. However, a similar logic as presented above for GRISM was used and an off-axis/spectral direction BSGF measurement is additionally performed. The configuration for such an off-axis is computed with the help of Zemax. The BSGF measurements comparison of same grating are presented in Figure 8. On the customer request, a third BSGF measurement is done keeping same solid angle for the detector all over the region of interest, up to 10° (green plot). The blue plot shows also presence of extra-features along the spectral direction, except the glitch around 2° only present on the right side, see in the Figure 8, which is an artifact from CASI S/W. Note that even for the 5° -off spectral plane measurement, some extra-features keep their BSGF value, around 1.5° and 6° , possibly suggesting the shape of a ring, as shown in the inset of Figure 8. Ideally, a 3D scanning when measuring grating's BSGF is preferred in order to map correctly all present extra-features.

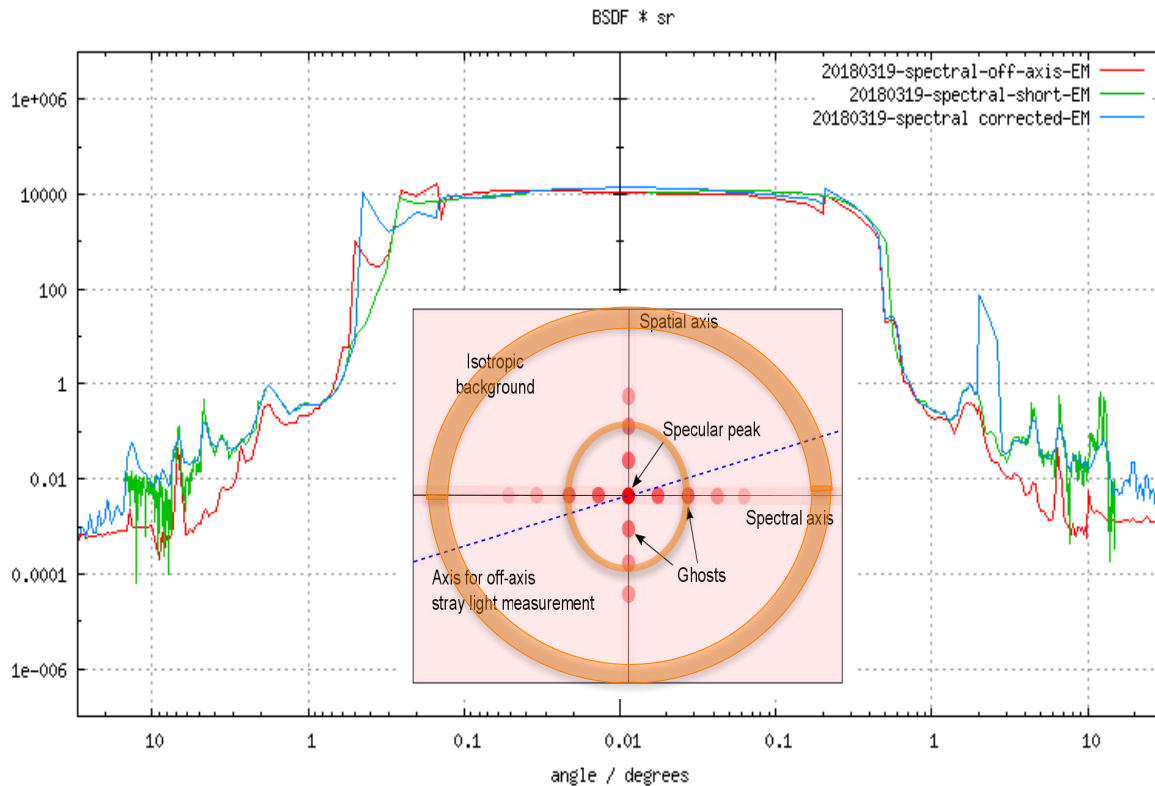


Figure 8. Immersed grating BSGF in spectral direction with different measurement configurations. The red-line plot represents the 5° off-axis measurement and is to be direct compared with the blue/green curves. The inset represents a schematic of a possible extra-features mapping, as generated by the immersed grating. Not all features have been suppressed when the measurement was performed in off-axis configuration.

3.3 Laser sources and band-pass filters

Scatter BSGF measurements performed on coatings or glasses/lenses do not require particular pure laser sources. When measuring gratings, due to their dispersive property, additional needs are imposed. Tube-lasers are preferred due to their emission line stability but the new technology developments of laser diodes (CW) makes them very attractive. The laser diodes e.g. Newport Velocity, have the advantage of being easy to purchase, are tunable lasers and provide a wider spectral range available. The samples under test presented in this paragraph are chosen to underline the importance of using a very stable and spectrally pure light source, eventually in combination with a band-pass filter.

The first example chosen here is a BSGF measurement of a grating using a HeNe laser tube using the emission line at 632.8nm wavelength. The grating is a flat grating and no aberrations are expected. The grating is of high quality showing a very low straylight level even close to specular. A band-pass filter with FWHM of 3nm was also used in front of the laser source to suppress eventually the residual secondary emission lines of the laser. While performing the grating

BSDF measurement, an asymmetric extra-feature present only on the left side was identified at about 0.6° , see Figure 9. Knowing the gratings parameters, the measurement configuration, and applying the grating equation⁷ for this specific alignment of the grating, the extra-feature was identified to be generated by the residual emission line, about 639.9nm. The grating dispersive property corroborated with high grating quality/low scatter straylight, allows the presence of both diffracted lines, at 632.8nm main and 639.9nm residual, to be mapped on same BSDF measurement. The assumption is checked and confirmed by measuring the BSDF of the same grating in same configuration using or not a band pass filter for 632,8nm, data shown in Figure 9. By measuring with and without a band-pass filter, it is clear that the asymmetric left side feature is an artifact of the set-up due to the secondary laser emission line (639.9) rather than an inherent feature of the grating and scales with the suppression factor of the filter used.

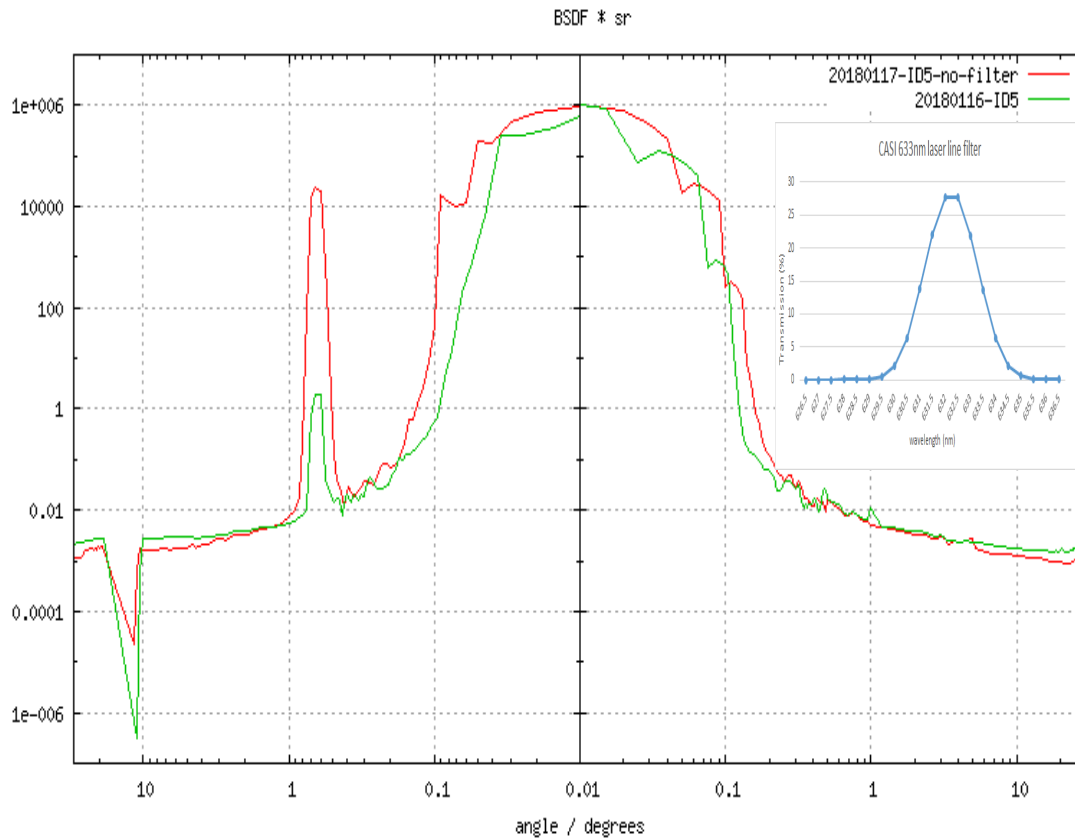


Figure 9. BSDF @632.6nm of a flat grating. The features on the left side of the spectra represent the secondary laser emission line diffracted by the grating, when using a BP filter (green plot) and without a BP filter (red plot).

Note that the band-pass filter used has a high attenuation factor suppressing the secondary emission line (at about 0.6°) by four orders of magnitude. The use of multiple band-pass filters would eventually suppress the HeNe laser secondary line completely, though at the cost of reducing the laser power, which would hamper the detection of very low diffracted/scattered power.

Similar approach was used when measuring an immersed grating (Si-based) at $2.377\mu\text{m}$ using a tunable diode Newport laser (Velocity TLB 6740). BSDF measurements were recorded using a band-pass filter NB5 (Omega Optical) for 2377nm. Figure 10 shows the BSDF measurements of the immersed grating, same configuration, when using the band-pass filter and without using it. The Figure 10 shows the BSDF measured only in the spectral direction. It can be noted that there is a higher scattered response of the grating when the band-pass filter is not filtering the laser, which fades away about 15° . The higher straylight level (scattering response) of the grating when measured without the selective filter is probably caused by emission of the source outside its main laser emission line. However both BSDF measurements show same extra-features in the spectral direction indicating that the features are not an artifact of the setup but rather features of the grating.

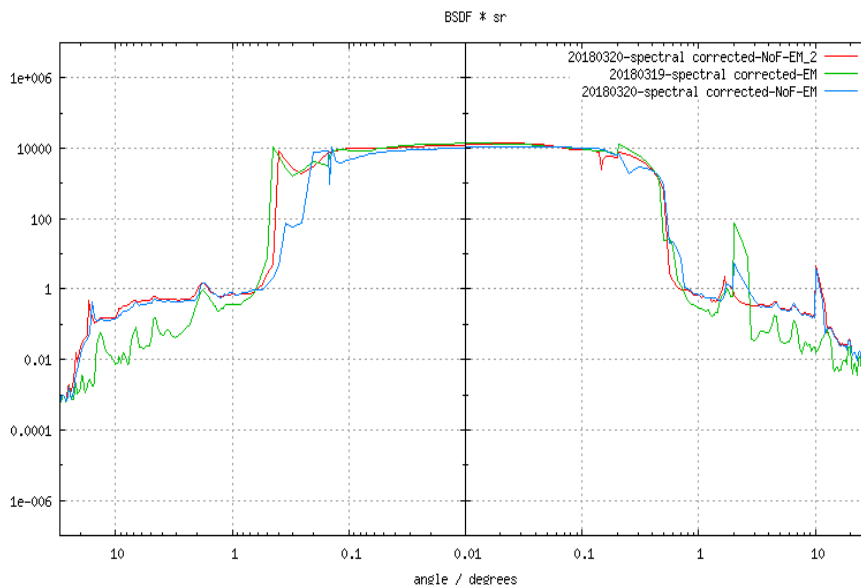


Figure 10. BSDF spectral configuration of a Si-based immersed grating at 2.377nm using the band-pass filter and without the band-pass filter (NoF).

4. CONCLUSIONS

We have presented different straylight measurements on gratings of complex geometry and at different wavelengths. For each BSDF measurement of the gratings, special configurations of the set-up were used. Near field measurements prove to be complex and limited mostly by the scatterometer capabilities. Most of the gratings measured and presented here do show extra features along the spectral direction and proved to be generated by the gratings. Only some of those extra features seem to be anisotropic, therefore present in all directions. Laser sources used in a scatterometer need to be careful selected and optimized by choosing a corresponding band-pass filter at the measurement wavelength.

5. ACKNOWLEDGEMENTS

The authors wish to thank all collaborators which have provided the different types of gratings and offer the opportunity to measure and characterize those complex optical elements: Horiba France SAS, Carl Zeiss Spectroscopy GmbH, SRON- Netherlands Institute for Space Research.

6. REFERENCE

- [1] Stover, J.C., [Optical Scattering, Measurements and Analysis, Third Edition], SPIE Press Book (2012)
- [2] <https://directory.eoportal.org/web/eoportal/satellite-missions/f/flex>
- [3] Coppo, P., Taiti, A., Pettinato, L., Francois, M., Taccola, M. and Drusch, M., “Fluorescence Imaging Spectrometer (FLORIS) for ESA FLEX Mission”, Remote Sens., 9, 649 (2017)
- [4] <https://www.sron.nl/earth-instrument-development/immersed-gratings>
- [5] Gulde, S.T., Kolm, M.G., Smith, D.G., Maurer, R., Bazalgette Courrèges-Lacoste, G., Sallusti, M., and Bagnasco M., “Sentinel 4: a geostationary imaging UVN spectrometer for air quality monitoring: status of design, performance and development”, ICSO 2014, 10563, 1056341-1056349 (2014)
- [6] <https://directory.eoportal.org/web/eoportal/satellite-missions/c-missions/copernicus-sentinel-5>
- [7] Palmer, C., [Diffraction Grating Handbook], 7-th Edition, Richardson Grating Newport Corporation; Ney-York, (2014) https://www.researchgate.net/publication/308402069_Diffraction_Grating_Handbook_7th_edition